Optical Measurement of Electron Spin Lifetimes in Gallium Arsenide

Dallas Carl Smith

A senior thesis submitted to the faculty of
Brigham Young University
in partial fulfillment of the requirements for the degree of

Bachelor of Science

John Colton, Advisor

Department of Physics and Astronomy

Brigham Young University

April 2011

ABSTRACT

Optical Measurement of Electron Spin Lifetimes in Gallium Arsenide

Dallas Carl Smith
Department of Physics and Astronomy
Bachelor of Science

We measured T_1 spin lifetimes for electrons in gallium arsenide at various magnetic field strengths. To perform these measurements, we initialized and probed the spin states using optical techniques. By changing the delay between the initializing (pump) and probe laser pulses, we traced out the spin polarization decay curves. From this data we extracted the T_1 spin lifetimes. This technique proved to be effective in measuring lifetimes in magnetic fields between 0 T and 7 T and at temperatures of 1.5 K and 5 K. Lifetimes in our sample were measured up to 800 ns.

Keywords: GaAs, Spin Lifetimes

ACKNOWLEDGMENTS

I would like to thank Brigham Young University for giving me the opportunity to obtain a greater understanding of physics and funding me while I completed these experiments. I would also like to acknowledge my advisor, Dr. John Colton, for never missing an opportunity to be an effective mentor. I am also grateful for his patience while I wrote this thesis. Most of all I would like to thank my sweet wife Natalie for always being supportive of my work and allowing me to spend the time necessary to complete this project.

Contents

Chapter 1

Introduction

1.1 Motivation

In the world today we rely increasingly on computers for data processing. In this context, increasing the computing power of modern electronics is a focus of research. Theoretical work showed the possibility of a quantum computer in 1985 [1], which would have the capability to solve certain types of problems in much fewer steps than a digital computer, thus significantly decreasing computation times. A classical computer uses a binary system of high and low states to store information called bits. The computer is able to store and manipulate the state of individual bits to process data. A quantum computer differs from classical computers in that it stores and processes information using quantum states. This gives it the potential to store information as "high" state, "low" state or a quantum mechanical superposition of both states. There are many types of quantum systems that could be used in quantum computers as quantum bits (called qubits). A great deal of current research investigates which of these systems would work best for this application [2].

David P. DiVincenzo [2] suggested that for a quantum computer to be plausible, five requirements must be met. There must be: (1) "a scalable physical system with well characterized qubits,"

(2) "The ability to initialize the state of the qubits," (3) "Long relevant decoherence times, much longer than the gate operation time," (4) "A 'universal' set of quantum gates," and (5) "A qubit-specific measurement capability." It has been proposed to use the spin of electrons for qubits [2]. Electron spin is a good candidate since it is a binary system (spin can be either up or down), and it is easily manipulated and observed. Lifetimes must be relatively long in order for electron spin states to be applicable to quantum computing. It is critical to understand and catalog spin lifetimes in various materials. This may help to achieve the third criterion in DiVincenzo's list.

I have focused my research exclusively on semiconductors, especially gallium arsenide (GaAs). Gallium arsenide is a particularly good material because of its optical properties. Two important optical properties are that it easily absorbs and emits light (see section 1.5), and that there are selection rules which connect the optical absorption to the spin states of the electrons. We determined spin lifetimes for electrons in a bulk sample of GaAs at various magnetic field strengths. Understanding spin lifetimes is a step in finding longer lifetimes, which will aid in the quest for practical quantum computers.

1.2 Lifetime Terminology

There are three types of spin lifetimes that are commonly measured. They are labeled T_1, T_2, and T_2^*.

When an electron is placed in a magnetic field, there is a split in the electron's energy levels known as the Zeeman effect which is governed by the equation

$$\Delta E = g\mu_B B \tag{1.1}$$

where ΔE is the split in energy levels, B is the external field, μ_B is the Bohr magneton, and g (called the g-factor) is a proportionality constant specific to the material. The spin has a tendency to align with the external field. The time this aligning process takes is commonly called the "spin

flip" lifetime because if the spin starts oriented opposite to the field then it is the characteristic time required for the spin to flip its direction. The spin-flip time (or longitudinal relaxation time) is referred to as the T_1 lifetime. This lifetime is typically the longest of the three lifetimes because unlike the other two, there must be a transfer in energy for the electron spin orientation to change its direction.

The T_2 lifetime is the transverse relaxation time. If an electron is placed in a magnetic field such that its spin angular momentum is perpendicular to the field, then the spin direction will precess about the field direction. If a group of electrons are aligned, an external field will cause the electrons to precess and get out of phase with respect to each other. Events such as phonon scattering can cause electrons to lose coherence. The characteristic time for this process is termed the T_2 or transverse lifetime. This quantity is the most important lifetime for quantum computing because it sets the maximum time for each operation in a quantum computing scheme. The T_2 lifetime is more difficult to measure than the T_1 lifetime since there is no change in the energy between the two states: in-phase compared with out-of-phase precession.

For inhomogeneous materials, the electron spins will precess at different rates, as a function of the location in the sample. This precession variation is due to an inhomogeneity of the electron g-factor. The T_2^* lifetime is a measurement of the "inhomogeneous dephasing" time, or the time required for the spins to get out of phase with each other in an inhomogeneous material. Because this time depends on both the inhomogeneity as well as the factors that produce T_2 lifetimes, T_2^* is the shortest of the three lifetimes and is a lower bound for the T_2 lifetime.

In the experiment that follows, we measured T_1 lifetimes.

1.3 Techniques

Most electron spin experiments require three steps. For simplicity, I will refer to the electron spin states as "spins." First, we initialize or put the spins into a particular state. Second, we manipulate the spins. Finally, we probe the spins. There are different methods to complete each of these three steps. Since it is possible to use different techniques for each of the steps, there are many types of spin experiments possible through the various combinations. Almost all of the spin-based experiments can be categorized in this way.

Initializing the spins in a particular, chosen state can be accomplished through a variety of techniques, such as electrical injection, the combination of a high magnetic field and low temperatures, or optical pumping. It is possible to electrically inject the spins into a sample in a preferred direction using spin light emitting diodes (this process is explained further in [3]). Under the right conditions, low temperature can also be used to initialize spins. The magnetic field must be high enough to cause substantial separation in the energy states and the temperature must be low enough to make the thermal promotions to higher energy levels less significant. Initializing spins can be done using optical methods as well. Photons interact with electrons, imparting to them their angular momentum, which causes the spins' orientation to change. Photons in circularly polarized light have angular momentum parallel to or anti-parallel to the direction of propagation (depending on the handedness of the polarization). Thus when a circularly polarized laser light interacts with a sample, some of the electrons in the materials will align in this direction. In our experiment, circularly polarized light is used to polarize electron spins.

After the spins have been initialized, they can be manipulated in various ways to learn about properties of the electrons. For instance, it is possible to use microwaves to drive the transition between spin states, a method called electron spin resonance (ESR). Using this technique we can

deduce the g-factor for the electrons in the material using the relationship

$$hf = g\mu_B B \tag{1.2}$$

where h is Plank's constant, f is the frequency of the applied microwaves, g is the g-factor, μ_B is the Bohr magneton, and B is the resonant magnetic field [4]. There are also some optical-only techniques to drive the transition between spin up and spin down using a pulsed laser with a specific spectrum [5]. In our experiment we simply wait for spins to naturally flip as a result of thermal relaxation.

Finally, probing spin states can be done many ways, but the discussion here will focus on optical techniques. Electrons can be probed optically by analyzing their photoluminescence. Spin-polarized electrons emit circularly polarized light when they fall to a lower energy state. The polarization of photoluminescence shows us the degree to which the electrons are polarized. Another optical method for probing electrons relies on Kerr rotation. When electrons in the conduction band are spin polarized, the absorption for one spin state will be different than that of another spin state. This causes a change in the index of refraction produced by the two spin states and hence seen by the two polarization directions of light relative to each other. This in turn causes linearly polarized light—which can be thought of as a linear superposition of the two circularly polarization helicities—to rotate its polarization angle as it transmits through the material or reflects off of the surface. For reflected light this is called the Kerr effect. To use the Kerr effect, linearly polarized light hits the sample with energy just high enough to interact with the electrons but not enough to promote them to the conduction band (meaning the photon's energy is just below the band gap of the material). The optical polarization of the reflected beam will be altered by the spin polarization of the electrons via the Kerr effect. Therefore, the degree of optical polarization rotation is proportional to the spin polarization. In this experiment we detected electron states by splitting the reflected beam from the sample into two orthogonal basis polarization to determine how much the linear polarization had rotated from its incident orientation.

1.4 Background

One of the most influential papers which marked the beginning of interest in GaAs spin lifetime research on spin lifetimes was written by Kikkawa *et al.*. In this paper the authors determined T_2^* lifetimes in different samples of GaAs, one of which exceeded 100 ns [6]. Since then a great effort has been made to measure all three spin lifetimes using a variety of samples and techniques. Many experiments have determined spin lifetimes in *n*-type GaAs.

We will now review three relevant papers measuring T_1 lifetimes of GaAs obtained for samples of different doping concentrations.

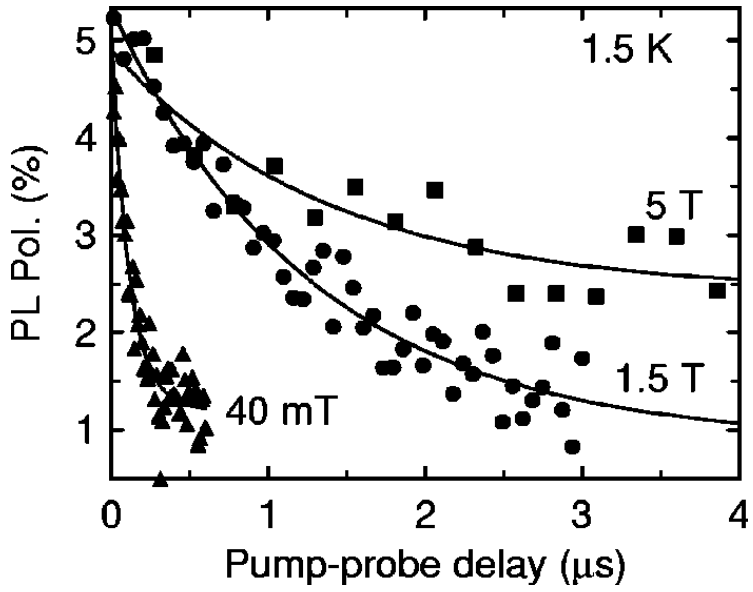

Figure 1.1 Polarization of electrons for various probe delays. The exponential decay is clear for each magnetic field. From Ref. [7]

In 2004, Colton *et al.* [7], performed measurements of T_1 lifetimes in *n*-type GaAs which was lightly doped (3×10^{15} extra electrons per cubic centimeter, denoted by 3E15 cm^{-3}). The authors initialized spins in the sample optically using a circularly polarized laser. This sample was then probed a short time later by measuring the photoluminescence stimulated by another laser pulse. The degree of emitted circular polarization was proportional to the degree of electron spin

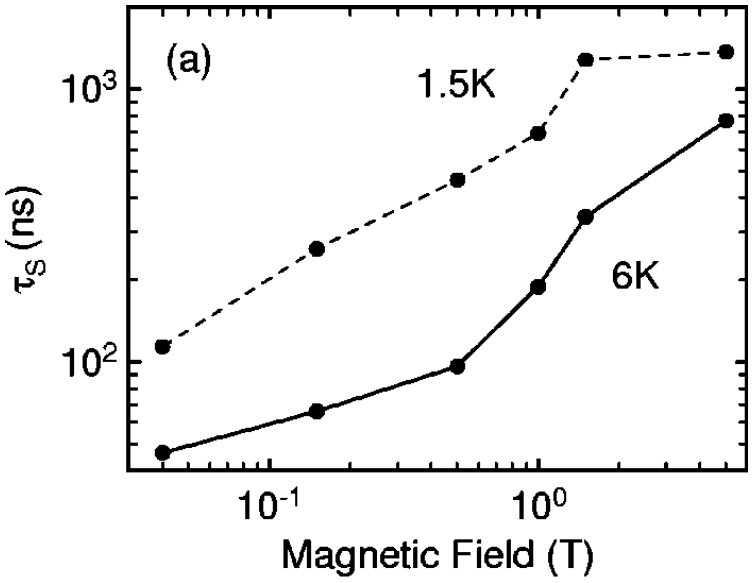

Figure 1.2 Spin lifetimes at different magnetic fields for 3E15 cm^{-3} doped sample at 1.5 and 5K. From Ref. [7]

.

polarization. By changing the delay between the pump and probe pulses they obtained a decay curve for the polarization of the electrons shown in Fig. 1.1.

After collecting this data for different magnetic fields, they plotted lifetime as a function of magnetic field strength, as seen in Fig. 1.2. The spin lifetimes increase with field as depicted in this figure. The maximum lifetime obtained in this study was about one microsecond.

In 2007, Colton *et al.* [8], measured T_1 spin lifetimes in a sample with a lower amount of doping (1E15 cm^{-3}). Using the same technique as in Ref. [7], the authors found that the magnetic field dependence had a slightly different shape, as seen in Fig. 1.3. The difference in behavior is attributed to the lower doping concentration. For that sample, lifetimes decrease as the field is taken above 2 T (for most temperatures) and increase again as the field is taken above 4 T. The maximum lifetime observed was 19 μs.

In 2006, Fu *et al.* [9] measured the spin lifetimes of GaAs at an even lower doping concentration (5E13 cm^{-3}). They used a method called photoluminescence excitation (PLE) to probe the electron

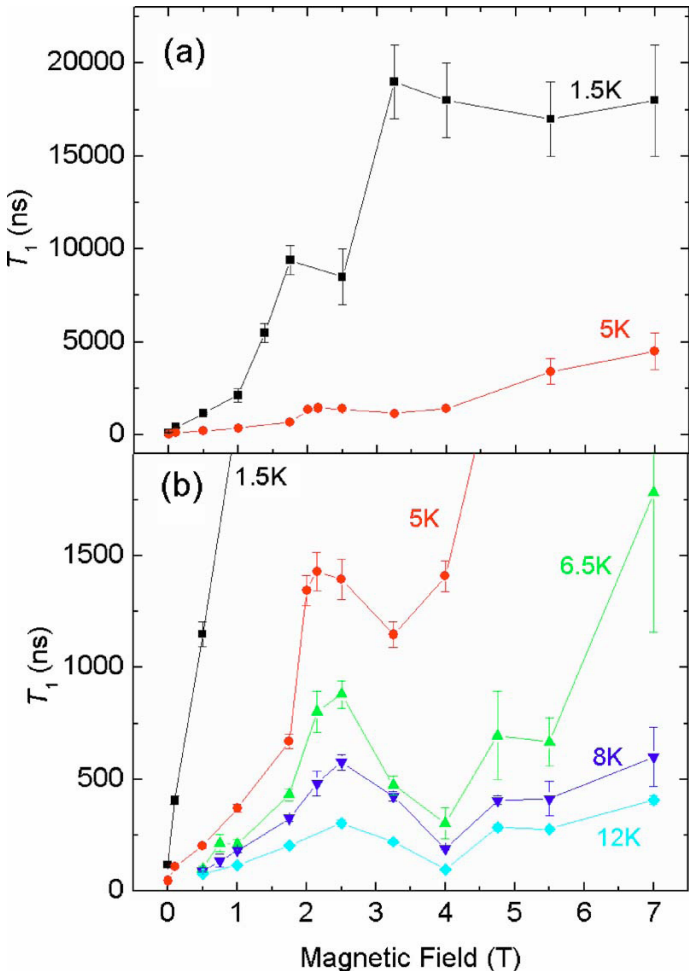

Figure 1.3 Spin lifetimes at different magnetic field for 1E15 cm^{-3} doped sample at various temperatures. This figure was taken from [8]

.

states by measuring the absorption of a spin-dependent transition. Their data, shown in Fig. 1.4, shows a very different behavior for the lifetime measurements. The measured lifetimes decrease as a function of the magnetic field for fields greater than 4 T, in contrast to previous studies. It should be noted that these experiments only provided a lower bound for measurements below 4 T since the experimental procedure did not allow accurate lifetime measurements in this region. The behavior for these lifetimes is exactly opposite of the behavior observed in the 1E13 cm^{-3} sample. Because

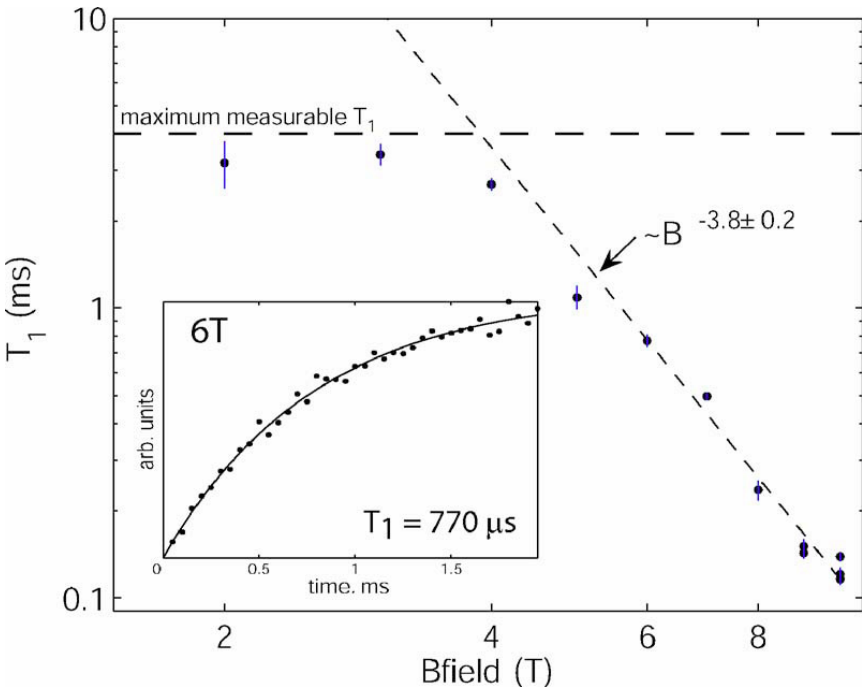

Figure 1.4 shows spin life times at different magnetic field for 5E13 cm^{-3} doped sample. From Ref. [9]

.

of this dramatic change in behavior, we are interested to learn how the spin lifetimes behave in the large gap between the doping levels 1E15 cm^{-3} and 5E13 cm^{-3} (see section 1.5).

1.5 Sample

Gallium arsenide has optical properties that make it ideal for spin applications. For instance, GaAs has a direct band gap. This means that it is able to absorb and emit photons without phonon interactions, which makes processes involving photon emission and absorption likely to occur. Indirect band gap materials like silicon are more difficult to study with optical techniques and use in optical applications.

We also chose to study *n*-type GaAs instead of *p*-type GaAs. An *n*-type semiconductor has

"extra" electrons while *p*-type semi-conductors have "extra" holes (missing electrons). Electrons in *p*-type semiconductors are actually more easily optically polarized than in *n*-type semiconductors. This is because electrons that exist in the conduction band can only be there as a direct result of optical excitation, therefore theoretically polarization could be 100%. We define polarization as

$$P = \frac{N_{lower} - N_{upper}}{N_{upper} + N_{lower}} \tag{1.3}$$

where N_{lower} is the number of electrons that are aligned with the magnetic field (i.e. are in the lower spin state), and N_{upper} is the number of electrons that are anti-aligned. Using Eqn. (1.3), we find that the polarization upon optical excitation will be 50% for GaAs since it populates these states in a 3:1 ratio [10]. *n*-type GaAs, on the other hand, already has non-spin-polarized electrons in the conduction band from the dopants. When optically pumping the spins the polarization increases from zero as pumping power is increased. In theory it may be possible to get 50% polarization with a strong enough pump, but in practice we are unable to achieve more than 20% polarization, and typically much less for *n*-type bulk GaAs. This fact might lead one to believe that *p*-type semiconductors would be a better material for these experiments. However, when electrons in the conduction band return to the valence band, they lose their polarization. This means that electron lifetimes depend on the length of time the electron is excited. This causes spin lifetimes to be very short for *p*-type semiconductors. Even though it is much more difficult to get a significant percentage of electrons polarized in *n*-type GaAs, the electrons that are polarized and promoted to the conduction band share their spin with other electrons in or near the conduction band through the fast exchange interaction. Therefore, even after the electron has fallen back to the valence band, there is a remnant of the polarization left in a "spin-reservoir" held by donor electrons. This allows *n*-type GaAs to have longer spin lifetimes than *p*-type GaAs and is why we chose to study *n*-type GaAs.

The doping of this sample was especially chosen to bridge a gap in the previous experiments. The doping level 3E14 cm^{-3} is of particular interest since it is close to the geometric mean of the

doping levels for the samples studied by Colton *et al.* [8] and Fu *et al.* [9] (see section 1.4).

Chapter 2

Experimental Setup

We measured T_1 spin lifetimes for GaAs in different magnetic fields using optical techniques. This chapter will begin by giving an overview of how the experiment works. Then it will describe in greater detail how we pump and probe the spin states. A description will then be given of how the data is collected. Fig. 2.1 shows the basic physical setup for the experiment.

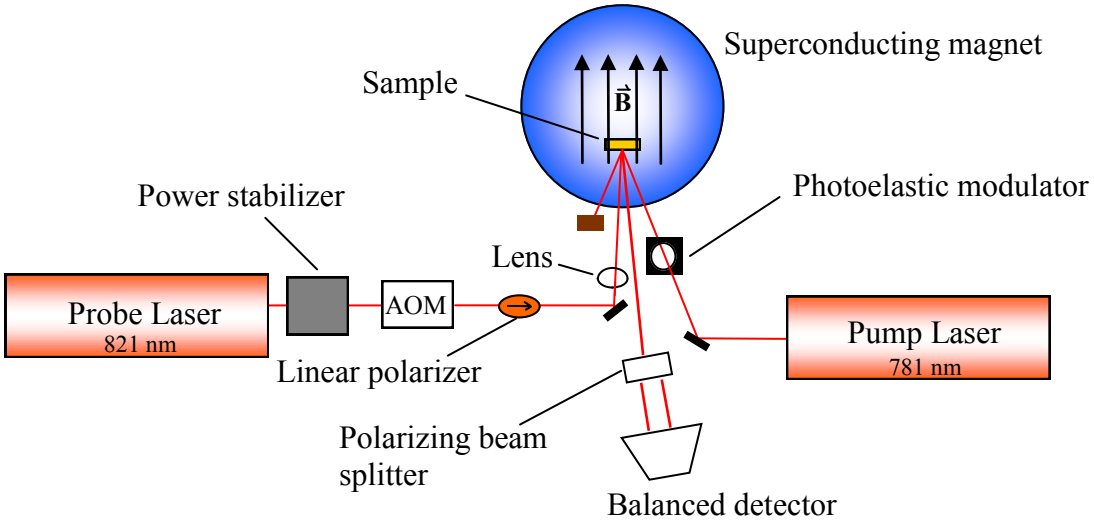

Figure 2.1 A simplified schematic of the experimental setup

2.1 Experimental Overview

The sample was positioned in a superconducting magnet, and it was cooled to a chosen low temperature using liquid helium. Then the magnet was set to a specific magnetic field. A small percentage of the electrons naturally align with the magnetic field. It can be shown using simple Boltzmann statistics that the polarization P is related to the magnetic field B through

$$P = \tanh\left(\frac{|g|\,\mu_B B}{2k_B T}\right) \tag{2.1}$$

where μ_B is the Bohr magneton, k_B is Boltzmann's constant, T is the temperature, and g is the electron g-factor—for GaAs $g \approx -0.44$. Equation (2.1) is derived in Appendix A. As an example at 1 T and 5 K, Eqn. (2.1) gives $P = 0.0246$. When we pump spin into the sample it adds or subtracts from this baseline polarization. In order to pump spins into the sample, we used circularly polarized laser pulses (pump beam). After a delay, the polarization of the spins was probed using a linearly polarized pulse from the probe laser. To determine the spin polarization, we measured the optical polarization of the reflected probe beam, which (via the Kerr effect) is proportional to the electron polarization. This measurement is referred to as the Kerr rotation and is described in section 1.3. This pump-probe sequence was repeated, and we gradually increased the delay between the two pulses. Plotting the Kerr rotation vs. the delay time revealed an exponential decay curve. From this information we extracted a spin lifetime. The whole process was then repeated for different magnetic fields and temperatures. The schematic of the experiment is represented in Fig. 2.1. Also shown in Fig. 2.2 is a diagram that shows timing in the experiment.

2.2 Initializing Spins

When photons from a circularly polarized laser interact with electrons in the sample, the photons impart some of their angular momentum to the electrons. This interaction aligns a portion of the

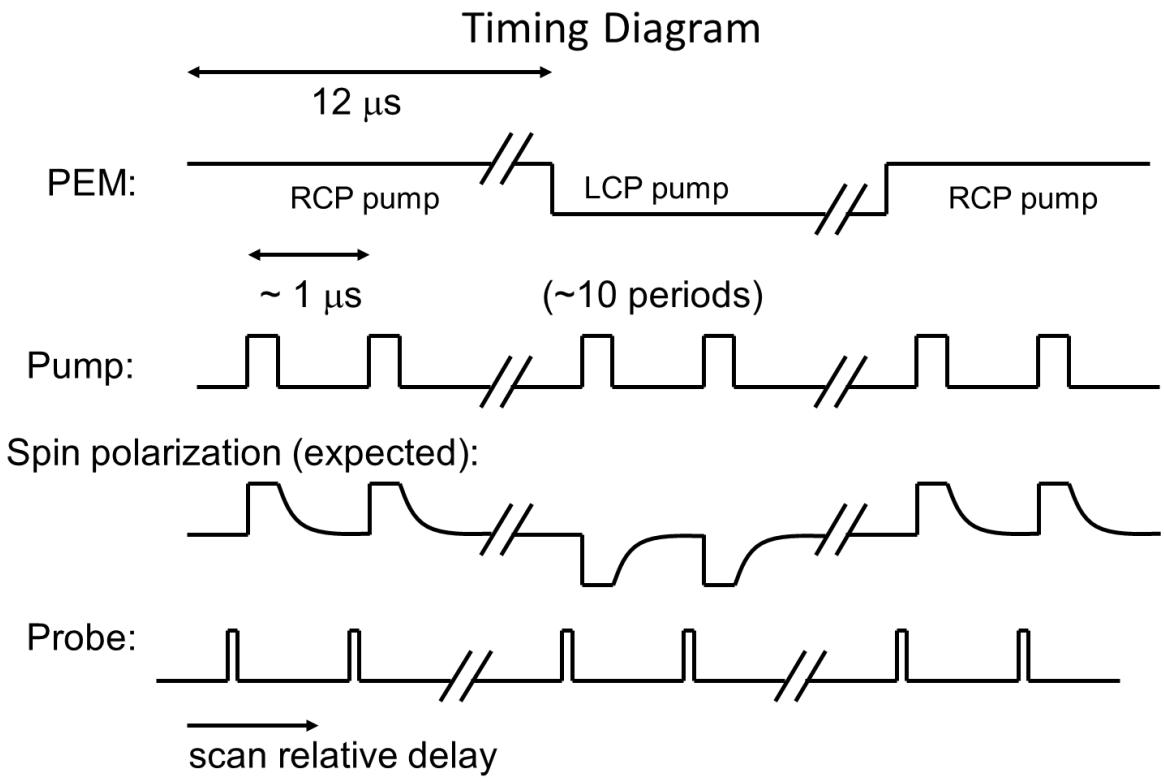

Figure 2.2 A diagram that shows relative pulse durations for the photoelastic modulator, pump laser pulse, probe laser pulse, and the expected spin decay.

spins in the sample (see section 1.3). We used a laser with circularly polarized light to initialize the spins. This laser is referred to as the pump laser. The pump laser we used is a Melles Griot diode laser with a wavelength of 781 nm and 21 mW of laser power. We chose this particular wavelength because it has energy just above the band gap of the GaAs, which is 818.5 nm. This allowed the electrons to absorb the photons and become polarized. The laser diode has a built-in power modulation mechanism. Using this mechanism to switch the laser on and off required a reference signal, which we provided with a pulse generator made by Agilent (model 81110A). Our pulse generator can output sequences of fast pulses to two instruments simultaneously with high timing accuracy.

As seen on the right side of Fig. 2.1, the pump laser beam first travels through a photoelastic modulator (PEM), which was made by Hinds Instruments. The PEM is a device that modulates between $\lambda/4$ retardance and $-\lambda/4$ retardance. It switches at a steady rate of 42 kHz. By using linearly polarized light oriented a 45° angle with respect to the fast axis of the PEM, we are able to modulate the pump laser between right-handed and left-handed polarized light at 42 kHz. The purpose for this practice is explained in section 2.4. The timing of the pump pulse and the PEM is shown in Fig. 2.2.

After the PEM, the pump laser beam is directed to the sample. We positioned the optics so that the laser hit the sample as close to normal incidence as possible. This orients the spins of the electrons parallel or anti-parallel to the magnetic field (depending on the handedness of the light), which is also perpendicular to the sample surface.

2.3 Probing Spins

An optical method was also used to probe the spin states in the sample. The probe laser was a tunable titanium-sapphire (Ti:Sapph) laser made by Spectra-Physics with the wavelength set to

821 nm. The selected wavelength was just below the band gap for GaAs (818.5 nm). This allowed the photons to interact with the electrons without changing the electron spin states.

The first instrument through which the probe beam traveled was a power stabilizer. This device employs an active feedback loop to constantly adjust the fraction of laser power that is let through to keep the output constant. The Ti:Sapph laser we used does not output a very stable power, thus it was important that we reduced its power variation. Having a stable probe laser helped reduce the noise in the signal.

Because our probe laser does not have a convenient modulation system built into it like the diode pump laser, it was necessary to use a different method to modulate the laser power. For this we used a device called an acousto-optic modulator (AOM). The AOM is capable of modulating the beam on and off fast enough to provide 20 ns pulses. The repetition rate for the probe beam was chosen so that the electrons would have sufficient time to decay before being polarized again by the next pump pulse. For most magnetic fields this was 1666 kHz, i.e. a 600 ns period. The probe pulse timing is shown in Fig. 2.2.

Following the AOM, the probe beam traveled through a linear polarizer in a rotational mount. This created a linearly polarized beam, the angle of which was adjusted to balance the signal before each scan. This process is described further in section 2.4.

After the linear polarizer, the beam was sent though a focusing lens to make the probe spot size at the sample just smaller than the pump spot size. When the two spots completely overlap, the probe beam will only probe areas that have been polarized by the pump beam. It is important to probe only areas in the pump beam spot since probing areas that were not initialized by the pump beam will decrease the polarization that we detect and may significantly decrease the signal to noise ratio. The method we use to measure the laser spot size is describe in appendix B. We oriented the probe laser so that it hit the sample as close to normal incidence as possible, just as we did for the pump laser.

There are many parameters in this experiment that needed to be adjusted in order to optimize the signal. One of these crucial parameters was the probe laser power. If the probe power was too low, then the measured signal would be small and the signal to noise ratio would be small. However, if the power of the probe pulse was too high, it would actually start changing the spins thus decreasing our signal. In order to determine the optimal power for the probe beam, we overlapped the pump and probe pulses in time and adjusted the probe power until the signal was at a maximum. In the most optimal configuration the probe laser is at 1.4 mW when it was on continuously. The overall period was chosen to be several T_1's long. A 3% duty cycle and a step size equal to half the probe pulse width then gave us 50 points per scan, or enough points to see the rise, decay, then baseline of the decay curves.

2.4 Collecting Data

Data was collected by analyzing the probe beam after reflecting off of the sample. Depending on the electron spin polarization, the linear polarization of the reflected beam rotated with respect to the incident polarization, an effect called the Kerr rotation (see section 1.3). To measure this rotation, we sent the reflected beam into a polarizing beam splitter—a device that spatially separates the reflected beam into vertically and horizontally polarized light. Both of these beams were sent into a balanced detector. A balanced detector consists of two detectors with an output that is the difference of two inputs. By measuring the subtracted signal we determined how much the polarization of the beam had rotated. Before we did a scan, we always "balanced" the detector by rotating the polarizer in the probe beam (while covering the pump beam) until the subtracted output was zero. As a result, the reflected beam had equal amounts of the two polarizations when it was not being pumped. We do this to reduce the noise in our data by removing the dc offset in the signal going to the lock-in amplifier. This process also reduces or eliminates "common made"

noise, noise which effects both channels equally (e.g. laser power fluctuations). The signal from the balanced detector represented a change in electron polarization.

There are a number of other effects that could cause electrons to lose polarization and could skew the spin lifetime measurements. An important example is thermal effects, specifically the heating caused by the pump beam. In order to subtract this factor out of our data and allow us to be more sensitive to the true signal we were interested in, we used a photoelastic modulator to vary the helicity of the pump beam combined with a lock-in amplifier referenced to that modulation frequency. This method allows us to see how the difference between aligning the spins parallel and anti-parallel to the field changes as we increase the time delay. Because heating will cause a decrease in polarization for both alignments, after looking at the difference in these two signals we are left with only the signal due to spin decay. The lock-in amplifier is a device that only measures the component of a signal that is at a given reference frequency. For this setup we used the 42 kHz frequency of the PEM. Using a lock-in amplifier allows us the capability of measuring signals from the detector as small as microvolts. Thus by using both the PEM and Lock-in, we are able to increase our signal by measuring only signal at the PEM frequency as well as subtract out unwanted effects from our data. The relative timing for each component in can be seen in Fig. 2.2.

Chapter 3

Results

3.1 Measurement of Lifetimes

We measured the electron spin lifetimes for GaAs at two temperatures and many different magnetic fields. In accordance with the theory, polarization of the electrons dropped off exponentially as the delay between the pump and probe increased. We plotted the relative polarization against the delay. Obtaining a spin lifetime from this data is just a matter of fitting a curve to the results. The final results of our experiments are modeled by the decaying exponential curve

$$P = Ae^{-t/T_1} + p_0 \tag{3.1}$$

where P is the spin polarization, t is time delay, and A, T_1 and p_0 are fitting parameters. When we have found the optimum fit for the data, T_1 is the measured lifetime. This is the time that we expect the polarization to drop to 37% $(1/e)$ of the initial polarization. Fig. 3.1 is representative of the data collected. The particular data set was taken at 1 T and 1.5 K using a 150 ns probe pulse, 200 ns pump pulse, and an overall period of 3500 ns. In the fit for this particular data we found that the spin lifetime was 414 ns. At all temperatures and magnetic field strengths the data followed the same basic shape. In each graph we have the expected spin decay beginning at or near time

$t = 500$ ns. This is when the probe beam temporally leaves the pump beam. The behavior of the data before the probe beam leaves the pump beam is not completely understood. In some scans the phase of the signal from the lock-in would shift when the beams were overlapped, but would then stay constant during the decay from a maximum polarization after the probe left the pump beam. We do not have a good explanation for this behavior although it happened consistently. Though this unexpected behavior is not understood, it seems clear that the decay portion of the graph is real spin decay.

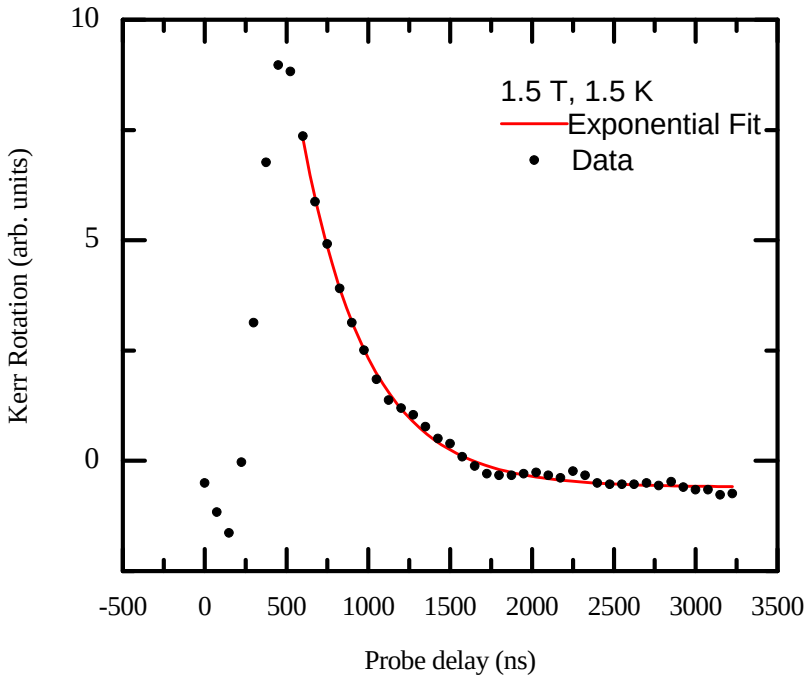

Figure 3.1 Scan at 1.5 K, 1.5 T. A clear decay curve can be seen on the right of the graph.

Another unexplained phenomenon came at fields greater that 6 T. In Fig. 3.2 the polarization of the sample appears to increase again at the tail of the polarization decay. This is an unexpected result because it suggests that the electrons are beginning to re-polarize without the pump beam. It is also possible that this could be a shift in the phase of the signal.

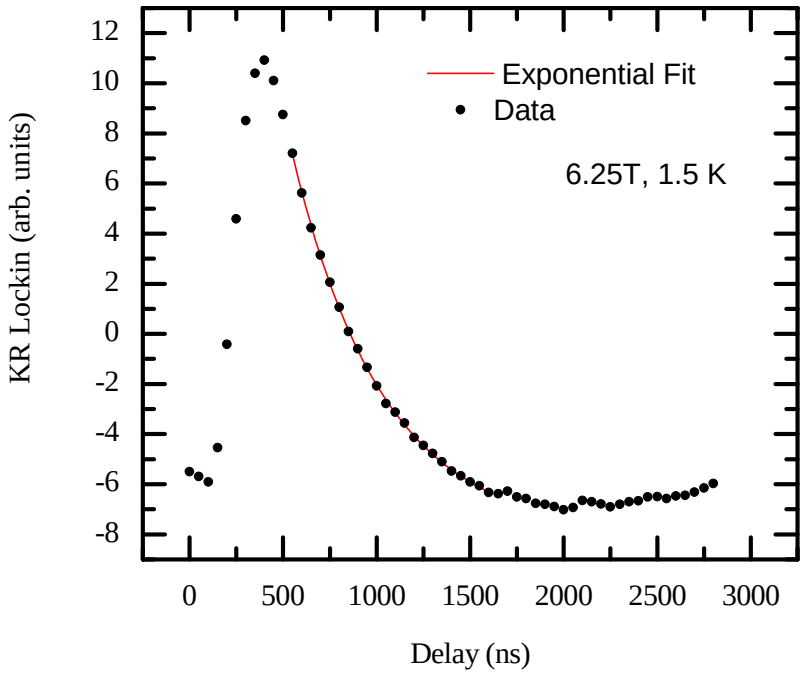

Figure 3.2 Scan at 1.5 K, 6.5 T. A decay curve with non-exponential tail.

3.2 Comparison to Previous Work

After we gathered the data, we fit an exponential curve for each scan to extract spin lifetimes. We then took all of the lifetime data and plotted it as a function of magnetic field strength. This is displayed in Fig. 3.3 and Fig. 3.4. We can see that the lifetimes generally increased with increased magnetic field. The sample more closely resembles the 3E15 cm^{-3} doped sample rather than the 5E13 cm^{-3} doped sample. There is also a clear dip in the lifetimes around 3.5 T for the 1.5 K data set. Another clear dip in the lifetimes for the 3E15 cm^{-3} sample occurs at a slightly different field strength. In the data gathered for this sample it occurs at 2.5 T for 1.5 K and at 3.5 T for 5 K. We are unsure of what mechanism caused this small decrease in our experiment, but it appears to be a real property.

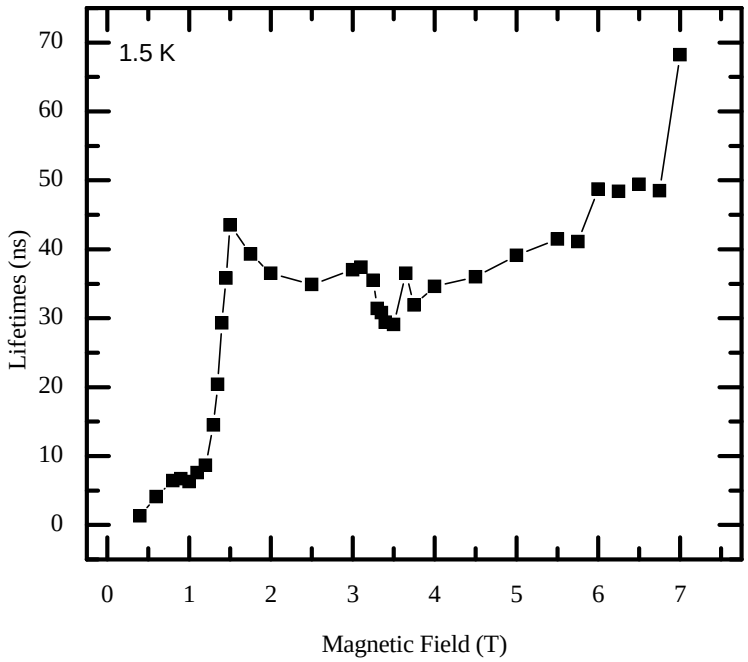

Figure 3.3 Spin lifetimes vs. magnetic field for our sample at 1.5 K

3.3 Uncertainty

The basic source of uncertainty in our data came from noise. When we fit an exponential curve to the data, this uncertainty was quantified by how well we were able to fit the data. When the noise seemed larger (especially at fields greater that 6 T and less that 1 T), we did two scans and averaged them to reduce this uncertainty.

One source of variation in our calculations came when fitting the curve to experimental data. We had a choice of which point to begin the fit. The lifetime would shift slightly based on which point we used as the first point in the fit. The time set on the pulse generator did not exactly correspond with the pulses arriving at the sample due to delays introduced in the AOM and the laser diode. We measured approximately how large these delays were with fast photodiode detector and an oscilloscope. Even with this knowledge it was sometimes difficult to choose the point with

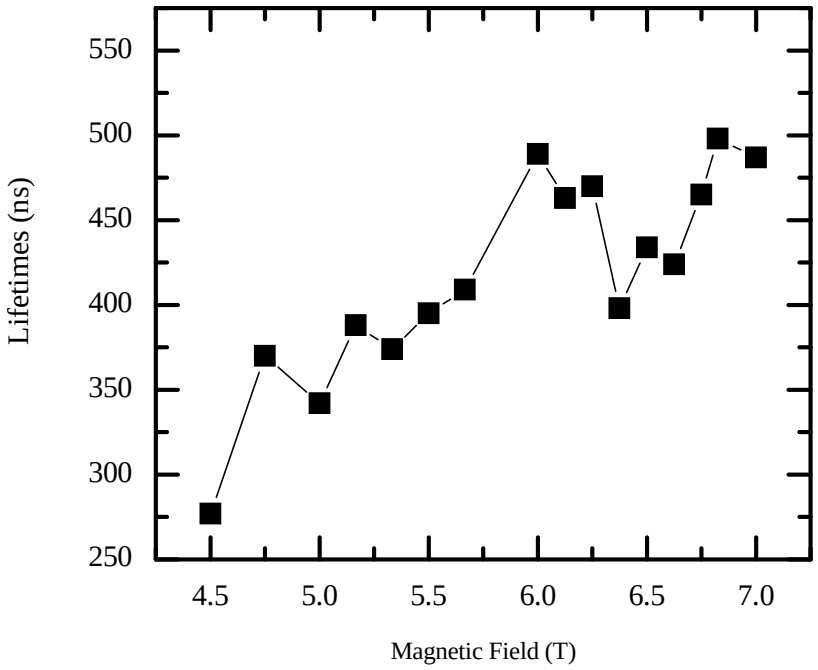

Figure 3.4 Spin lifetimes vs. magnetic field for our sample at 5 K

which to start the fit. In most instances, the uncertainty caused by these two factors was usually no more than 20 ns for the longest T_1 measurement.

We were careful to keep both of the lasers blocked when we were not running scans; however, because the laser remained on during the scans, it could potentially have polarized the nuclei. The effective magnetic field created by the polarized nuclei could affect the spin lifetimes. This could also be another source of variation in our data.

3.4 Conclusion and Future Outlook

When no magnetic field is present, we expect that T_1 spin lifetimes are approximately the same as T_2^* because there is no energy difference for the electron's orientation. The lifetime in this region

is limited by in homogeneous dephasing caused by the precession around the effective magnetic field caused by the spin of the nuclei in the sample. When an external field becomes greater than the effective field created by the nuclei, the spin lifetime should begin to sharply increase. This happens because the external field creates a splitting of the electron's energy levels much larger than the hyperfine splitting that comes from the nuclei spin interaction. This effect can only be observed at very low fields and might be what is seen in Fig. 3.3 at fields less than 1 T. It is difficult to measure lifetimes in this region because they are so short. The lower limit of the lifetimes that we can measure is set by the length of the smallest probe pulse, which was 20 ns in our experiment.

In accordance with previous work done on GaAs discussed in section 1.4, we can see that the lifetimes we measured increase as the magnetic field increases for the lower magnetic fields. An explanation for this phenomenon is discussed by D'yakonov *et al.* [11], who predicts that $1/T_1$ should follow a Lorentzian shape. This effect is governed by the correlation time τ_c, which describes the time required for electrons to interact with each other. This correlation time τ_c has been predicted for GaAs at different temperatures and doping concentrations [11]. D'yakonov's analysis would predict the shape of $1/T_1$ should follow

$$\frac{1}{T_1} \propto \frac{1}{B^2 + B_c^2} \tag{3.2}$$

where $B_c = \hbar/\tau_c \mu_B g$. Since everything in this equation is constant except B, it shows that the lifetime should increase with an increase in magnetic field. For our data, $1/T_1$ data taken below 1.3 T very loosely follows a Lorentzian shape which would give a correlation time of $\tau_c = 2.8$ ns.

The D'yakonov theory breaks down at higher fields due to the fact that correlation times are actually not constants, but vary with magnetic field. At extremely high fields, the electrons become more localized and will thus interact less with each other. This will cause the correlation time to decrease, making it a less important factor. In this regime other factors dominate the interaction and the result is that the lifetimes will drop sharply with an increase in magnetic fields. For an understanding of the theory of this phenomenon see D'yakonov's description in [11]. We were not

able to take our magnetic field high enough to see this effect, but it can clearly be seen in Fig. 1.4.

The lifetimes we measured increased with magnetic field as expected. The previous papers indicated a trend that when doping was decreased, lifetimes increased for GaAs at 1.5 K [7] [8] [9]. However, the lifetimes were shorter than this trend would predict. The mechanism that causes this is still unclear.

We will continue further investigation of this sample. We plan to repeat this experiment to check the reproducibility of the data. Also, we need to gather more data on the temperature dependence of the lifetimes. At higher temperatures we would expect these lifetimes to be even shorter. Studying many more doping concentrations using this technique will make a more complete picture of how doping affects spin lifetimes.

Although some of the results cannot be explained, we learned a lot about the measurement process. One conclusion we can draw from this experiment is that the technique that was used is effective in determining spin lifetimes. Though some of the electron measurements were difficult to understand, it is likely that the method that we used did provide us with data portraying real polarization decay. Thus the method described will be a powerful tool for measuring spin lifetimes in future studies.

Appendix A

Polarization Derivation

In this appendix we will use Maxwell-Boltzmann statistics to derive Eqn. 2.1.

Equation 1.3 defines polarization to be the difference between the proportions of electrons in the upper state and in the lower state. Thus

$$P = \frac{N_{lower}}{N_{total}} - \frac{N_{upper}}{N_{total}} \tag{A.1}$$

Maxwell-Boltzmann Statistics tell us that

$$\frac{N_i}{N_{total}} = \frac{e^{-\varepsilon_i/k_B T}}{Z} \tag{A.2}$$

where ε_i is the energy of the ith state, k_B is Boltzmann's constant, T is the temperature and Z is the partition function

$$Z = \sum_i e^{-\varepsilon_i/k_B T} \tag{A.3}$$

For the two state system we are working with the energy of the two states is the split in energy caused by the external magnetic field. The total separation of energy levels for the electrons in these two states is a result of the Zeeman effect (Eqn. 1.1). We chose to reference the energy with respect to the midpoint of this separation, thus our two resulting energy levels are

$$\varepsilon_{upper} = \frac{|g|\,\mu_B B}{2} \tag{A.4}$$

$$\varepsilon_{lower} = -\frac{|g|\,\mu_B B}{2} \tag{A.5}$$

where g is the electron g-factor and μ_B is the Bohr magneton. Now if we combine all of the above equations we find

$$P = \frac{N_{lower}}{N_{total}} - \frac{N_{upper}}{N_{total}}$$

$$= \frac{e^{-\varepsilon_{lower}/k_B T} - e^{-\varepsilon_{upper}/k_B T}}{Z}$$

$$= \frac{e^{-\varepsilon_{lower}/k_B T} - e^{-\varepsilon_{upper}/k_B T}}{e^{-\varepsilon_{lower}/k_B T} + e^{-\varepsilon_{upper}/k_B T}}$$

$$= \frac{e^{|g|\mu_B B/2k_B T} - e^{-|g|\mu_B B/2k_B T}}{e^{|g|\mu_B B/2k_B T} + e^{-|g|\mu_B B/2k_B T}}$$

$$P = \tanh\left(\frac{|g|\,\mu_B B}{2k_B T}\right) \tag{A.6}$$

which is the equation for polarization (Eqn. 2.1)

Appendix B

Measuring Laser Spot Size

It was essential to the experiment to know what the two spot sizes were for the two laser beams since the pump beam needed to be a little larger than the probe beam. In order the measure the size of the beams we set up a razor blade on a micrometer at the position we needed to determine the beam diameter. Using the micrometer we stepped the razor blade though the beam while measuring how the laser power decreased using a power meter as we gradually blocked the laser. We then plotted the laser power vs micrometer position and differentiated this graph to obtain a beam profile. Using the computer program Origin, we were able to fit a gaussian function to the profile and then find the length of +/- one standard deviation. For a gaussian, this is half width at $1/e^2$ peak power which is the effective radius of the beam. Using this value we calculate the area of the spot at the position of the razor blade. We could not actually position the razer blade at the sample position since this would require moving the magnet. Using linear extrapolation we were able to estimate the spot size at the sample by using measurements of the beam radius at two locations in front of the sample. Using this method we compared both spot sizes and were able to position the lens in such a way that the probe beam spot area was a little smaller than the pump beam spot area.

Bibliography

[1] D. Deutsch, "Quantum Theory, the Church-Turing Principle and the Universal Quantum Computer," Proceedings of the Royal Society of London. Series A, Mathematical and Physical Sciences **400,** 97–117 (1985).

[2] D. P. DiVincenza, "The Physical Implementation of Quantum Computation," Fortscher Phys **40,** 9–11 (2000).

[3] R. Fiederling, M. Keim, G. Reuscher, W. Ossau, G. Schmidt, A. Waag, and L. W. Molenkamp, "Injection and detection of a spin-polarized current in a light-emitting diode," Nature **402,** 787–790 (1999).

[4] J. S. Colton, T. A. Kennedy, A. S. Bracker, D. Gammon, and J. B. Miller, "Optically oriented and detected electron spin resonance in a lightly doped n-GaAs layer," Physical Review B **67,** 165315 (2003).

[5] D. Press, T. D. Ladd, B. Zhang, and Y. Yamamoto, "Complete quantum control of a single quantum dot spin using ultrafast optical pulses," Nature **456,** 218–221 (2008).

[6] J. M. Kikkawa and D. D. Awschalom, "Resonant Spin Amplification in n-Type GaAs," Physical Review Letters **80,** 19 (1998).

[7] J. Colton, T. Kennedy, and D. Gammon, "Microsecond spin-flip times in n-GaAs measured by time-resolved polarization of photoluminescence," Physical Review B **69,** 121307 (2004).

[8] J. S. Colton, M. E. Heeb, P. Schroeder, A. Stokes, L. R. Wienkes, and A. S. Bracker, "Anomalous magnetic field dependence of the $T1$ spin lifetime in a lightly doped GaAs sample," Phys. Rev. B **75,** 205201 (2007).

[9] K.-M. C. Fu, W. Yeo, S. Clark, C. Santori, C. Stanley, M. C. Holland, and Y. Yamamoto, "Millisecond spin-flip times of donor-bound electrons in GaAs," Physical Review Letters B **74,** 121304 (2006).

[10] B. Zakharchenya and F. Meier, *Optical Orientation, Modern Problems in Condensed Matter Sciences* (Elsevier Science Ltd, 1984).

[11] M. I. D'yakonov and V. I. Perel', Sov. Phys. **JETP 38,** 177 (1974).

Index